Sources of Chemicals. [^{3}H]SCH 23390 was synthesized as described previously.[49] [^{3}H]spiperone was purchased from New England Nuclear (Boston, MA). The following drugs were obtained as gifts: SCH 23390 (Schering Inc., Bloomfield, NJ), quinpirole (Eli Lilly, Indianapolis, IN), ketanserin tartrate (Janssen Pharmaceutica, New Brunswick, NJ), and SKF 38393 and chlorpromazine (Smith, Kline and French, Philadelphia, PA). All other compounds were purchased from commercial sources.

Acknowledgment. This work was supported by PHS Grants MH42705, MH40537, ES01104, Center Grants HD03310, MH133127, and Training Grant GM07040. We thank Dr. Mark Foreman, of Eli Lilly and Co., for helpful comments and preliminary data during the early phases of this research, and Dr. Andrew J. Hoffman for assistance with the conformational energy calculations.

Registry No. **4a**, 126295-91-8; **4a**·HCl, 126327-49-9; **4b**, 126295-92-9; **4b**·HBr, 126295-93-0; **4c**, 126295-94-1; **4c**·HBr, 126295-95-2; **5**, 126295-96-3; **5**·HBr, 126295-97-4; **6**, 126295-98-5; *cis*-**7**, 126295-99-6; *trans*-**7**, 126296-00-2; *cis*-**8**, 126296-01-3; *trans*-**8**, 126296-02-4; **9a**, 126296-03-5; **9a**·HCl, 126296-04-6; **6b**, 126296-05-7; **9b**·HCl, 126296-06-8; **10**, 126296-07-9; **11**, 126296-08-0; **12**·HCl, 126296-09-1; **13a**·HCl, 126296-10-4; **13b**, 126296-11-5; **13b**·HCl, 126296-12-6; **13c**, 126296-13-7; **13c**·HCl, 126296-14-8; **17**, 126296-15-9; **17**·HBr, 126296-16-0; $PhCH_2NH_2$, 100-46-9; CH_3CH_2CHO, 123-38-6; benzaldehyde, 100-52-7; 6,7-dimethoxy-β-tetralone, 2472-13-1; 6,7-dimethoxy-β-tetralone *N*-benzyl enamine derivative, 126296-17-1; *N*-benzyl-6,7-dimethoxy-1,2,3,4-tetrahydro-2-naphthylamine hydrochloride, 126296-18-2.

(48) Lowry, O. H.; Rosebrough, N. J.; Farr, A. L.; Randall, R. J. *J. Biol. Chem.* **1951**, *193*, 265.
(49) Wyrick, S.; McDougald, D. L.; Mailman, R. B. *J. Labeled Compd. Radiopharm.* **1986**, *23*, 685.

Structure–Activity Relationships for Metal-Labeled Blood Flow Tracers: Comparison of Keto Aldehyde Bis(thiosemicarbazonato)copper(II) Derivatives

Elizabeth K. John and Mark A. Green*

Department of Medicinal Chemistry and Pharmacognosy, School of Pharmacy, Purdue University, West Lafayette, Indiana 47907. *Received September 26, 1989*

Radiocopper-labeled pyruvaldehyde bis(N^4-methylthiosemicarbazonato)copper(II), Cu[PTSM], is under investigation as a radiopharmaceutical for evaluation of regional blood flow in the brain, heart, and kidneys because it affords relatively high levels of radioactivity in these organs upon intravenous injection, followed by prolonged tissue retention of the radiolabel. To probe and differentiate the physicochemical properties that are critical for blood–brain barrier (BBB) penetration and tissue retention in complexes of this type, 17 ^{67}Cu-labeled copper(II) bis(thiosemicarbazone) derivatives of Cu[PTSM] have been prepared and characterized, focusing on the bis(thiosemicarbazone), bis(N^4-methylthiosemicarbazone), bis(N^4-dimethylthiosemicarbazone), and bis(N^4-ethylthiosemicarbazone) derivatives of several alkylglyoxals ($R_{(l)}$ = Me, Et, *n*-Pr, *i*-Pr, *n*-Bu, or Me(EtO)CH) and phenylglyoxal. The compounds studied varied in lipophilicity from log P = 0.75 to log P = 3.5 (where P is the octanol/water partition coefficient). In rat biodistribution studies the N^4-methylthiosemicarbazone ($R_{(l)}$TSM) and N^4-dimethylthiosemicarbazone ($R_{(l)}TSM_2$) complexes always show comparable cerebral uptake at 1 min postinjection (iv) for any given $R_{(l)}$ group, while the thiosemicarbazone ($R_{(l)}$TS) complex always penetrates the BBB less efficiently. Comparison of the various Cu[$R_{(l)}$TS] derivatives shows that their brain uptake does tend to increase with increasing lipophilicity over the range 0.75 < log P < 2.4, although it never reaches that of the N^4-alkylated derivatives. The Cu[$R_{(l)}$TS] and Cu[$R_{(l)}$TSM] complexes are found to exhibit prolonged cerebral retention of activity, consistent with their known susceptibility to reductive decomposition by intracellular sulfhydryl groups, while the more inert Cu[$R_{(l)}TSM_2$] complexes clear from the brain relatively rapidly. Tracer clearance kinetics in the heart and kidney are similar to those observed for the brain with each of the tracers examined.

Introduction

Radionuclide imaging remains a technique that uniquely addresses the frequent need of the medical community for measurements of tissue perfusion at the capillary level. However, despite the importance of perfusion imaging, especially in the diagnosis of cardiovascular[1-3] and cerebrovascular[4,5] disease, the ability of nuclear medicine to provide this information often remains limited by the radiopharmaceuticals that are now available. A radiotracer that is completely extracted from blood into tissue in its first pass through the capillary system will map regional perfusion and will also allow calculation of absolute regional blood flow (mL min^{-1} g^{-1}), if both the tissue concentration of tracer and the concentration of tracer in the arterial blood supplied to the organ are known.[6]

Radiolabeled microspheres, sized such that they will be mechanically trapped in the capillary bed of an organ, serve as one standard to which possible new blood flow agents can be compared.[7] Biodegradable denatured albumin particles (macroaggregated albumin or MAA) that can be labeled[8-10] with ^{99m}Tc, ^{68}Ga, or ^{11}C are routinely used in the clinical assessment of pulmonary blood flow following intravenous injection. Unfortunately, the use of particulate tracers to evaluate perfusion in other organs

* Author to whom correspondence should be addressed.

(1) Rozanski, A.; Berman, D. S. *Semin. Nucl. Med.* **1987**, *17*, 104–120.
(2) Schelbert, H. R. *Semin. Nucl. Med.* **1987**, *17*, 145–181.
(3) Geltman, E. M.; Bergmann, S. R.; Sobel, B. E. In *Positron Emission Tomography*; Reivich, M., Alavi, A., Eds.; A. R. Liss: New York, 1985; Chapter 20, pp 345–385.
(4) Wood, J. H., Ed. *Cerebral Blood Flow*; McGraw-Hill: New York, 1987.
(5) Knezevic, S., Maximilian, V. A., Mubrin, Z., Prohovnik, I., Wade, J., Eds. *Handbook of Regional Cerbral Blood Flow*; L. Erlbaum: Hillsdale, NJ, 1988.
(6) Lacombe, P.; Meric, P.; Seylaz, J. *Brain Res. Rev.* **1980**, *2*, 105–169.
(7) Warner, D. S.; Kassell, N. F.; Boarini, D. J. In *Cerebral Blood Flow*; Wood, J. H., Ed.; McGraw-Hill, New York, 1987; pp 288–298.
(8) Davis, M. A. In *Radiopharmaceuticals*; Subramanian, G., Rhodes, B. A., Cooper, J. F., Sodd, V. J., Eds.; Society of Nuclear Medicine: New York, 1975; pp 267–281.
(9) Wilson, R. A.; Shea, M. J.; Landsheere, C. M.; Turton, D.; Brady, F.; Dearfield, J. E.; Selwyn, A. P. *Circulation* **1984**, *70*, 717–723.
(10) Even, G. A.; Green, M. A. *Nucl. Med. Biol.* **1989**, *16*, 319–321.

0022-2623/90/1833-1764$02.50/0

Scheme I. Synthesis and Structural Formula of Bis(thiosemicarbazone) Ligands and Copper(II) Chelates

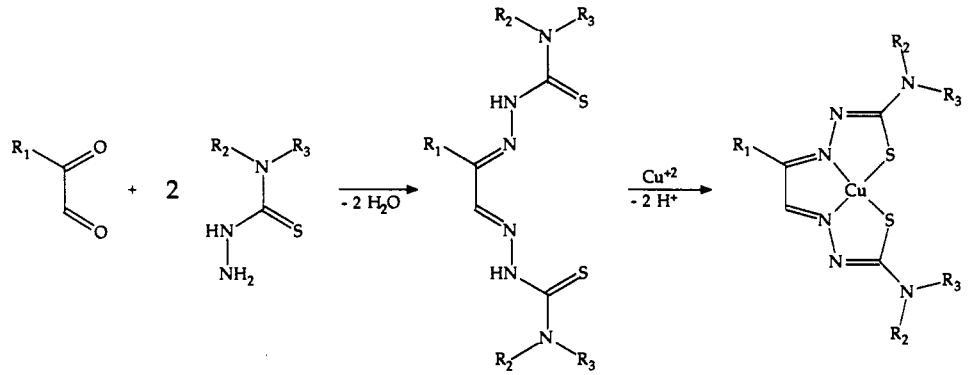

requires the microspheres be administered directly into the arterial circulation (e.g. by catheterization to allow left ventricular injection), an invasive procedure that is undesirably complex for widespread routine clinical use. The problems associated with the use of labeled microspheres to evaluate regional blood flow can be avoided by use of soluble tracers that, following intravenous administration, can diffuse freely from blood into tissues of interest.[6,11,12]

The best radiopharmaceuticals now available for making *quantitative* regional perfusion measurements in the living body are labeled with short-lived positron-emitting nuclides that can be imaged by positron emission tomography (PET).[13,14] The short half-lives of available positron emitters permits relatively large doses of activity to be safely administered to patients without excessive radiation exposure, allowing perfusion images to be obtained in a relatively short imaging time. In addition, the rapid decay of these nuclides facilitates repeat imaging procedures after only brief delays. Quantitative PET measurements of blood flow in the brain and heart can be obtained with diffusible tracers, like [^{11}C]-1-butanol or [^{15}O]water, by using a mathematical model to determine regional perfusion from the measured tissue and arterial blood activities.[13-20] Unfortunately, facilities for PET imaging with these tracers remain confined to a relatively few large medical centers capable of supporting the in-house biomedical cyclotron required to produce the very short-lived radiolabels.

The availability of positron-emitting radiopharmaceuticals labeled with an isotope that can be obtained from a parent/daughter generator system could facilitate more widespread use of PET by reducing or eliminating the need for a hospital cyclotron.[21,22] The decay of zinc-62 produces a positron-emitting copper-62 daughter.[23] The 9.8-min half-life of the latter is well-suited to the time frame of a PET perfusion study while remaining long enough to potentially allow the synthesis of a variety of copper-labeled radiopharmaceuticals. However, the development of metal-labeled radiopharmaceuticals for the study of cerebral perfusion has been an especially difficult problem in radiopharmaceutical chemistry,[24] since high cerebral extraction of tracer requires the compound efficiently penetrate the blood–brain barrier (BBB). The physicochemical properties that a compound must possess, if it is to freely diffuse across the blood–brain barrier, have not been completely defined. It is well-documented that molecules should be uncharged and lipophilic if they are to partition from blood through the capillary endothelial cell membrane and into the brain.[12,24-31] Dischino has measured the single-pass cerebral extraction for a series of carbon-11 labeled alcohols and ethers in a baboon model and correlated the results with compound lipophilicity.[31] At a cerebral blood flow of 1.0 mL min^{-1} g^{-1}, complete cerebral extraction was observed for compounds with $0.9 < \log P < 2.5$ (where P = the octanol/water partition coefficient). As lipophilicity increased above $\log P = 2.5$, cerebral extraction was increasingly diminished, presumably because of competitive nonspecific binding of these highly lipophilic compounds to plasma proteins or other blood components.

(11) Rose, C. P.; Goresky, C. A. In *Handbook of Physiology: The Cardiovascular System*; American Physiological Society: Bethesda, MD 1984; Section 2, Volume IV, Part 2, pp 781–798.
(12) Fenstermacher, J. D.; Rapoport, S. I. In *Handbook of Physiology: The Cardiovascular System*, American Physiological Society: Bethesda, MD 1984; Section 2, Volume IV, Part 2, pp 969–1000.
(13) Reivich, M., Alavi, A., Eds. *Positron Emission Tomography*; A. R. Liss: New York, 1985.
(14) Phelps, M., Mazziota, J., Eds. *Positron Emission Tomography and Autoradiography: Principles and Applications for the Brain and Heart*; Raven Press: New York, 1986.
(15) Hack, S. N.; Eichling, J. O.; Bergmann, S. R.; Welch, M. J.; Sobel, B. E. *J. Clin. Invest.* **1980**, *66*, 918–927.
(16) Bergmann, S. R.; Fox, K. A. A.; Rand, A.; McElvaney, K. D.; Welch, M. J.; Markham, J.; Sobel, B. E. *Circulation* **1984**, *70*, 724–733.
(17) Herscovitch, P.; Markham, J.; Raichle, M. E. *J. Nucl. Med.* **1983**, *24*, 782–789.
(18) Raichle, M. E.; Martin, W. R. W.; Herscovitch, P.; Mintum, M. A.; Markham, J. *J. Nucl. Med.* **1983**, *24*, 790–798.
(19) Raichle, M. E. In *Shortlived Radionuclides in Chemistry and Biology*; Rost, J. W., Krohn, K. A., Eds.; American Chemical Society: Washington, D.C., 1981; 419–436.
(20) Ter-Pogossian; Herscovitch, P. *Semin. Nucl. Med.* **1985**, *15*, 377–194.
(21) Robinson, G. D. In *Positron Emission Tomography*; A. R. Liss: New York, 1985; Chapter 4, pp 81–101.
(22) Welch, M. J.; Kilbourn, M. R.; Green, M. A. *Radioisotopes (Japan)* **1985**, *34*, 170–179.
(23) Lederer, C. M.; Shirley, V. S., Eds. *Table of Isotopes*, 7th ed.; J. Wiley: New York, 1978.
(24) Oldendorf, W. H. *J. Nucl. Med.* **1978**, *19*, 1182.
(25) Oldendorf, W. H. *Proc. Soc. Exp. Biol. Med.* **1974**, *147*, 813–815.
(26) Oldendorf, W. H. Molecular Criteria for Blood–brain Barrier Penetration. In *Noninvasive Brain Imaging: Computed Tomography and Radionuclides*; DeBlanc, H. J., Sorenson, J. A., Eds.; Soc. Nucl. Med.: New York, 1975.
(27) Levin, V. A. *J. Med. Chem.* **1980**, *23*, 682–684.
(28) Crone, C. C.; Levitt, D. G. Capillary Permeability to Small Solutes. In *Handbook of Physiology, Section 2, The Cardiovascular System*; Rankin, E. M., Michel, C. C., Eds.; American Physiological Society: Bethesda, MD 1984; Vol. IV, 411–466.
(29) Fenstermacher, J. D. Drug Transfer Across the Blood–brain Barrier. In *Topics and Pharmaceutical Sciences 1983*; Breimer, D. D., Speiser, P., Eds.; Elsevier: New York, 1983.
(30) Young, R. C.; Mitchell, R. C.; Brown, T. H.; et al. *J. Med. Chem.* **1988**, *31*, 656–671.
(31) Dischino, D. D.; Welch, M. J.; Kilbourn, M. R.; Raichle, M. E. *J. Nucl. Med.* **1983**, *24*, 1030–1038.

We have previously shown in animal models that the copper(II) complex of pyruvaldehyde bis(N^4-methylthiosemicarbazone), Cu[PTSM], efficiently crosses the blood–brain barrier.[32,33] This copper-labeled agent shows promise as a perfusion tracer for the brain, heart, and kidneys, affording relatively high concentrations of activity in these organs upon intravenous injection, followed by prolonged "microsphere-like" retention of tissue radiocopper.[32-37] To probe and differentiate the physicochemical properties that are critical for blood–brain barrier penetration and tracer retention, we have now prepared and studied 17 ^{67}Cu-labeled copper(II) bis(thiosemicarbazone) complexes related to Cu(PTSM).

Experimental Section

Thiosemicarbazide, N^4-methylthiosemicarbazide, N^4-ethylthiosemicarbazide, and pyruvaldehyde were obtained from Aldrich Chemical Co. N^4,N^4-Dimethylthiosemicarbazide,[38,39] 2--keto-3-ethoxybutyraldehyde,[40] and phenylglyoxal[41] were obtained by literature methods.

Ethylglyoxal, *n*-propylglyoxal, isopropylglyoxal, and *n*-butylglyoxal were prepared by following a general literature procedure.[42] Briefly, the appropriate 2,2-dichloroaldehyde was obtained by chlorination of the corresponding aldehyde in DMF at 70–90 °C. The 2,2-dichloro aldehyde in methanol was then treated with sodium methoxide to yield the 2,2-dimethoxy aldehyde, which was then hydrolyzed in 5% H_2SO_4 without isolation to give the desired alkylglyoxal derivative.

Pyruvaldehyde bis(thiosemicarbazone),[43] pyruvaldehyde bis(N^4-methylthiosemicarbazone),[44] pyruvaldehyde bis(N^4-dimethylthiosemicarbazone),[45] pyruvaldehyde bis(N^4-ethylthiosemicarbazone),[46] ethylglyoxal bis(thiosemicarbazone),[47] ethylglyoxal bis(N^4-methylthiosemicarbazone),[48] ethylglyoxal bis(N^4,N^4-dimethylthiosemicarbazone),[49] 2-keto-3-ethoxybutyraldehyde bis(thiosemicarbazone),[50] 2-keto-3-ethoxybutyraldehyde bis(N^4-methylthiosemicarbazone),[51] 2-keto-3-ethoxybutyraldehyde bis(N^4,N^4-dimethylthiosemicarbazone),[52] *n*-propylglyoxal bis(thiosemicarbazone),[53] *n*-propylglyoxal bis(N^4-methylthiosemicarbazone),[54] isopropylglyoxal bis(thiosemicarbazone),[55] isopropylglyoxyal bis(N^4-methylthiosemicarbazone),[56] *n*-butylglyoxal bis(thiosemicarbazone),[57] *n*-butylglyoxal bis(N^4-methylthiosemicarbazone),[58] phenylglyoxal bis(thiosemicarbazone),[59] and

(32) Green, M. A. *Nucl. Med. Biol.* **1987**, *14*, 59–61.
(33) Green, M. A.; Klippenstein, D. L.; Tennison, J. R. *J. Nucl. Med.* **1988**, *29*, 1549–1557.
(34) (a) Barnhart, A. J.; Voorhees, W. D.; Green, M. A. *J. Nucl. Med.* **1989**, *30*, 848. (b) Barnhart, A. J.; Voorhees, W. D.; Green, M. A. *Nucl. Med. Biol.* **1989**, *16*, 747–748.
(35) (a) Shelton, M. E.; Green, M. A.; Mathias, C. J.; Welch, M. J.; Bergmann, S. R. *J. Nucl. Med.* **1989**, *30*, 768. (b) Shelton, M. E.; Green, M. A.; Mathias, C. J.; Welch, M. J.; Bergmann, S. R. *J. Nucl. Med.* **1989**, *30*, 1843–1847.
(36) (a) Shelton, M. E.; Green, M. A.; Mathias, C. J.; Weinheimer, C. J.; James, H. L.; Welch, M. J.; Bergmann, S. R. *J. Nucl. Med.* **1989**, *30*, 807. (b) Shelton, M. E.; Green, M. A.; Mathias, C. J.; Welch, M. J.; Bergmann, S. R. *Circulation*, submitted for publication.
(37) (a) Mathias, C. J.; Welch, M. J.; Green, M. A.; McGuire, A. H.; Perry, D. J.; Raichle, M. E.; Lich, L. L.; Zinn, K. R. *J. Nucl. Med.* **1989**, *30*, 791. (b) Mathias, C. J.; Welch, M. J.; Raichle, M. E.; Mintun, M. A.; Lich, L. L.; McGuire, A. H.; Zinn, K. R.; John, E.; Green, M. A. *J. Nucl. Med.* **1990**, *31*, 351–359.
(38) McElhinney, R. S. *J. Chem. Soc.* **1966**, 950–954.
(39) Audrieth, L. F.; Scott, E. S.; Kipper, P. S. *J. Org. Chem.* **1954**, *19*, 733.
(40) Rappen, L. *J. Prakt. Chem.* **1941**, *157*, 177.
(41) Rabjohn, N. *Org. React.* **1949**, *5*, 331.
(42) (a) Debuyck, L.; Verhē R.; Dekimpe, N.; Schamp, N. *Bull. Soc. Chim. Belg.* **1980**, *89*, 441. (b) Verhē, R.; Courtheyn, D.; Dekimpe, N.; Debuyck, L.; Schamp, N. *Synthesis* **1982**, *8*, 667.
(43) Physical data for H_2[PTS]: mp 248–249 °C dec; FAB mass spectrum for $C_5H_{10}N_6S_2$ shows an MH^+ peak at 219. IR (KBr): 1600 (C=S) cm^{-1}. NMR (90 MHz, DMSO-d_6): δ 2.15 (s, 3 H CCH_3), 7.65 (s, H, CH), 7.7–7.9 (broad, NH_2) 8.1–8.3 (broad, NNH).
(44) Physical data for H_2[PTSM]: mp 231–323 °C dec; FAB mass spectrum for $C_7H_{14}N_6S_2$ shows an MH^+ peak at 247. IR (KBr): 1520 (C=S) cm^{-1}. NMR (90 MHz, DMSO-d_6): δ 2.2 (s, 3 H CCH_3), 3.05 (d, J = 4.5 Hz, 6 H, NCH_3) 7.7(s, H, CH) 8.3–8.6 (broad, 2 H, N-H), 10.4 (s, H, NH), 11.8 (s, H, NH).
(45) Physical data for H_2[$PTSM_2$]: mp 151–152 °C dec; FAB mass spectrum for $C_9H_{18}N_6S_2$ shows an MH^+ peak at 275. IR (KBr): 1500 (C=S) cm^{-1}. NMR (90 MHz, DMSO-d_6): δ 2.10 (s, 3 H, CCH), 3.25 (s, 12 H, $N(CH_3)_2$), 7.85 (s, H, CH).
(46) Physical data for H_2[PTSE]: mp 220 °C dec; FAB mass spectrum for $C_7H_{14}N_4S_2$ shows an MH^+ peak at 247. IR (KBr): 1500 (C=S) cm^{-1}, NMR (90 MHz, DMSO-d_6): δ 1.15 (t, J = 5.0 Hz, 3 H, N-CH_3) 1.4–1.7 (m, 2 H, $-NCH_2$), 2.20 (s, 3 H, CCH_3), 7.50 (s, H, -CH) 8.40–8.60 (broad, 2 H, NH).
(47) Physical data for H_2[ETS]: mp 232–236 °C dec; FAB mass spectrum for $C_6H_{12}N_6S_2$ shows an MH^+ peak at 233. IR (KBr): 1600 (C=S) cm^{-1}. NMR (90 MHz, DMSO-d_6): δ 0.95 (t, J = 7.0 Hz, 3 H, $-CH_3$), 2.60 (q, J = 6.0 hZ, 2 H, $-CH_2$), 7.6 (s, H, CH) 7.70–7.90 (broad, NH_2) 8.05–8.35 (broad, NNH).
(48) Physical data for H_2[ETSM]: mp 212–213 °C dec; FAB mass spectrum for $C_8H_{16}N_6S_2$ shows an MH^+ peak at 261. IR (KBr): 1500 (C=S) cm^{-1}. NMR (90 MHz, DMSO-d_6): δ 1.00 (t, J = 7.0 Hz, 3 H, CH_3), 2.80 (q, J = 7.0 Hz, 2 H, CH_2), 3.05 (d, J = 7.0 Hz, 6 H, NCH_3), 7.55 (s, H, CH), 8.3–8.6 (broad, 2 H, NH).
(49) Physical data for H_2[$ETSM_2$]: FAB mass spectrum for $C_{10}H_{20}N_6S_2$ shows an MH^+ peak at 289. IR (KBr) 1500 (C=S) cm^{-1}. NMR (90 MHz, DMSO-d_6): δ 1.50 (t, J = 7.0 Hz, 3 H, $-CH_3$) 2.90 (q, J = 7.0 Hz, 2 H, $-CH_2$), 3.30 (s, 12 H, $N(CH_3)_2$), 7.85 (s, H, CH).
(50) Physical data for H_2[KTS]: mp 203–205 °C dec; FAB mass spectrum for $C_8H_{16}N_6S_2O$ shows an MH^+ peak at 277. IR (KBr): 1600 (C=S) cm^{-1}.
(51) Physical data for H_2[KTSM]: mp 201–202 °C (dec; FAB mass spectrum for $C_{10}H_{20}N_6S_2O$ shows an MH^+ peak at 305. IR (KBr): 1500 (C=S) cm^{-1}.
(52) Physical data for H_2[$KTSM_2$]: mp 139–140 °C dec; FAB mass spectrum for $C_{12}H_{24}N_6S_2O$ shows an MH^+ peak at 333. IR (KBr): 1500 (C=S) cm^{-1}.
(53) Physical data for H_2[*n*-PrTS]: mp 205–206 °C dec; FAB mass spectrum for $C_7H_{14}N_4S_2$ shows an MH^+ peak at 247. IR (KBr): 1600 (C=S) cm^{-1}. NMR (90 MHz, DMSO-d_6): δ .90 (t, J = 8.0 Hz, 3 H, $-CH_3$), 1.2–1.6 (m, 2 H, $-CH_2$) 2.8 (t, J = 9.0 Hz, 2 H, $-CH_2$), 7.65 (s, H, -CH), 7.7–7.9 (broad, NH_2), 8.25–8.45 (broad, NNH).
(54) Physical data for H_2[*n*-PrTSM]: mp 175–176 °C dec; FAB mass spectrum for $C_9H_{18}N_6S_2$ shows an MH^+ peak at 275. IR (KBr): 1550 (C=S) cm^{-1}. NMR (90 MHz, DMSO-d_6): δ 0.90 (t, J = 8.0 Hz, 3 H, $-CH_3$), 1.2–1.7 (m, 2 H, $-CH_2$), 2.75 (t, J = 9.0 Hz, 2 H, $-CH_2$), 3.00 (d, J = 5.4 Hz, 6 H, N, $-CH_3$, 7.60 (s, H, -CH), 8.15–8.35 (broad, NH).
(55) Physical data for H_2[*i*-PrTS]: mp 188–189 °C dec; FAB mass spectrum for $C_7H_{14}N_6S_2$ shows an MH^+ peak at 247. IR (KBr): 1600 (C=S) cm^{-1}. NMR (90 MHz, DMSO-d_6): δ 1.15 (d, J = 9.0 Hz, 6 H, $-C(CH_3)_2$), 2.8–3.2 (m, H, -CH), 7.5–7.8 (broad, NH), 7.80 (s, H, CH), 8.05–8.45 (broad, NNH).
(56) Physical data for H_2[*i*-PrTSM]: mp 192–193 °C dec; FAB mass spectrum for $C_9H_{18}N_6S_2$ shows an MH^+ peak at 275. IR (KBr): 1550 (C=S) cm^{-1}. NMR (90 MHz, DMSO-d_6): 1.10 (d, J = 9.0 Hz, 6 H, $-C(CH_3)_2$), 2.5–2.9 (m, H, -CH) 2.95 (d, J = 5.4 Hz) 6 H, NCH_3) 7.1–7.5 (broad, NH), 7.75 (s, H, -CH), 7.9–8.1 (broad, NNH).
(57) Physical data for H_2[n-BuTS]: mp 224–225 °C dec; FAB mass spectrum for $C_8H_{16}N_6S_2$ shows an MH^+ peak at 261. IR (KBr): 1600 (C=S) cm^{-1}. NMR (90 MHz, DMSO-d_6) δ 0.85 (t, J = 9.0 Hz, 3 H, $-CH_3$), 1.0–1.5 (m, 4 H, $-CH_2$), 2.80 (t, J = 9.0 Hz, 2 H, $-CH_2$), 7.60 (s, H, -CH), 7.70–8.00 (broad, NH) 8.2–8.6 (broad, NNH).
(58) Physical data for H_2[n-BuTSM]: mp 177–178 °C dec; FAB mass spectrum for $C_{10}H_{20}N_6S_2$ shows an MH^+ peak at 289. IR (KBr): 1500 (C=S) cm^{-1}. NMR (90 MHz, DMSO-d_6): δ 0.90 (t, J = 9.0 Hz, 3 H, $-CH_3$), 1.20–1.50 (m, 4 H, $-CH_2$), 3.00 (d, J = 5.2 Hz, 6 H, *n*-CH_3), 7.60 (s, H, -CH), 8.2–8.4 (broad, NH), 8.5–8.80 (broad, NNH).
(59) Physical data for H_2[PhTS]: mp 223–224 °C dec; FAB mass spectrum for $C_{10}H_{12}N_6S_2$ shows an MH^+ peak at 281. IR (KBr: 1600 (C=S) cm^{-1}. NMR (90 MHz, DMSO-d_6): δ 7.90 (s, H, CH) 7.2–7.8, 8.0–8.7 (m C_6H_5, NH).

phenylglyoxal bis(N^4-methylthiosemicarbazone)[60] were obtained by condensation of the keto aldehyde with the corresponding thiosemicarbazide derivative following the general procedure described in the literature[61] (Scheme I).

Copper-67 was obtained in high specific activity (>10^5 Ci/mol) as copper(II) in HCl solution from either Los Alamos or Brookhaven National Laboratory and used within 3 weeks of receipt. The [^{67}Cu]copper(II) bis(thiosemicarbazone) complexes were prepared as described previously.[33] Briefly, to the acidic ^{67}Cu solution was added pH 5 acetate buffer followed by an ethanolic sodium hydroxide solution containing an excess of the bis(thiosemicarbazone) ligand. The amount of NaOH used in a given preparation was determined by the amount required to approximately neutralize the quantity of HCl present. Formation of the [^{67}Cu]copper(II) bis(thiosemicarbazone) complex occurs essentially in the time of mixing. The product was then diluted to a salt concentration suitable for intravenous injection, while an ethanol concentration of 5–10% was maintained, and the final solution was filtered through a 0.2-μm sterile polytetrafluoroethylene membrane disposable filter unit before use.

The radiochemical purity of the ^{67}Cu-labeled complexes was verified by thin-layer chromatography on silica gel plates eluted with ethyl acetate.[32,33] The resulting radiochromatograms were analyzed with a Berthold Tracemaster 20 Automatic TLC Linear-Analyzer. With this TLC system the copper(II) bis(thiosemicarbazone) complexes migrate with R_f = 0.46–0.94, while ionic copper remains at the origin. Octanol/water partition coefficients were measured by vortex mixing 1 mL of 1-octanol and 1 mL of isotonic Tris buffer (pH 7.0)[62] with a 1–5-μL sample of the radiolabeled aqueous copper complex. Following centrifugation at >1200g for 5 min, the octanol and aqueous phases were sampled and counted in an automatic well counter (Packard Autogamma 5530) using a window centered on the 185 keV ^{67}Cu gamma peak. Partition coefficients, P, are reported as counts per gram of octanol divided by counts per gram of water.

The biodistribution of each copper tracer was determined following a 0.2-mL (1–3 μCi) injection with a 27-gauge needle into the femoral vein of ether-anesthetized Sprague-Dawley rats (generally 175–225 g). The injected solutions contained 5–10% ethanol to insure solubility of the lipophilic copper complexes. Syringes were weighed on an analytical balance before and after injection to precisely determine the dose administered to each rat. Ether-anesthetized animals were sacrificed by decapitation at given time intervals postinjection, relevant organs were excised, blotted to remove surface blood, and weighed, and ^{67}Cu levels were measured with the automatic gamma counter. Tissue distributions expressed as percent injected dose per gram (wet weight) and percent injected dose per organ were calculated by using counts from an aliquot of a weighed and appropriately diluted standard dose. Total blood volume was assumed to be 7% of total body mass. Generally four rats were studied at each time point for each compound; the results are reported as mean ± standard deviation. The percent injected dose/gram tables provided as supplementary material specify the number of animals averaged for each data point as well as the mass range of the animals studied for each compound. Some of the data for the pyruvaldehyde and ethylglyoxal derivatives has been reported previously[33,63] but is tabulated again here to facilitate comparisons with the remaining tracers.

Results and Discussion

Keto aldehyde bis(thiosemicarbazone) ligands are attractive for use in the development of copper-labeled radiopharmaceuticals for perfusion imaging, since they afford highly stable, uncharged, and relatively low molecular weight copper(II) complexes. In addition, due to the antineoplastic activity exhibited by some derivatives (notably Cu[KTS]), extensive literature already exists documenting their chemical fate in biological systems.[64–68] Complexes of this type have stability constants on the order of 10^{18} at physiological pH[65,66] and are kinetically quite stable in the absence of sulfhydryl reductants.[64–68] (The cytotoxicity of the copper(II) bis(thiosemicarbazone) complexes should pose little concern at the very low tracer concentrations of material that will be accessible with no-carrier-added copper-62).

While the 10-min half-life of copper-62 is attractive for PET perfusion imaging, it is undesirably short for laboratory research. Therefore, we have employed longer lived copper-67 ($t_{1/2}$ = 65 h) in order to screen radiocopper complexes to identify the most promising radiopharmaceuticals for labeling with copper-62. We report here the results obtained with 17 ^{67}Cu-labeled copper(II) bis(thiosemicarbazone) complexes related to Cu[PTSM], focusing on the bis(thiosemicarbazone), bis(N^4-methylthiosemicarbazone), and bis(N^4-dimethylthiosemicarbazone) derivatives of several alkylglyoxals and phenylglyoxal (Scheme I and Table I). We also examined the bis(N^4-ethylthiosemicarbazone) derivative of pyruvaldehyde. The copper-67 complex of each ligand was obtained in >95% radiochemical yield as assessed by thin-layer chromatography. The procedure employed for the synthesis of these radiotracers could readily be adapted to use with the eluent of the ionic ^{62}Cu generator described by Robinson.[69]

The lipophilicity of these compounds increases as expected with increasing alkyl substitution of the π-conjugated ligand backbone (Table I). Since the presence of even traces of ionic radiocopper impurities that would be confined to the aqueous phase could very markedly affect the magnitude of the partition coefficients measured by our technique for the more lipophilic tracers, the octanol phase was routinely repartitioned with a fresh aqueous

Table I. Copper(II) Keto Aldehyde Bis(thiosemicarbazone) Complexes Studied[a]

ligand	R_1	R_2	R_3	M_r	log P
PTS	methyl	H	H	280	0.76 ± 0.04
PTSM	methyl	Me	H	308	1.92 ± 0.04
$PTSM_2$	methyl	Me	Me	336	3.18 ± 0.05
PTSE	methyl	Et	H	336	2.76 ± 0.05
ETS	ethyl	H	H	294	1.35 ± 0.02
ETSM	ethyl	Me	H	322	2.65 ± 0.07
$ETSM_2$	ethyl	Me	Me	350	3.32 ± 0.04
KTS	Me(EtO)CH	H	H	338	1.71 ± 0.04
KTSM	Me(EtO)CH	Me	H	366	2.64 ± 0.11
$KTSM_2$	Me(EtO)CH	Me	Me	394	3.46 ± 0.15
n-PrTS	n-propyl	H	H	308	1.78 ± 0.05
n-PrTSM	n-propyl	Me	H	336	2.86 ± 0.02
i-PrTS	iso-propyl	H	H	308	1.82 ± 0.02
i-PrTSM	iso-propyl	Me	H	336	2.77 ± 0.01
n-BuTS	n-butyl	H	H	322	2.30 ± 0.03
n-BuTSM	n-butyl	Me	H	350	3.16 ± 0.12
PhTS	phenyl	H	H	342	2.37 ± 0.05
PhTSM	phenyl	Me	H	370	3.06 ± 0.15

[a] Functional substituents (R) numbered as in Scheme I.

(60) Physical data for H_2[PhTSM]: mp 178–179 °C dec; FAB mass spectrum for $C_{12}H_{16}N_6S_2$ shows an MH^+ peak at 309. IR (KBr): 1550 (C=S) cm^{-1}. NMR (90 MHz, DMSO-d_6): δ 3.00 (d, J = 5.5 Hz, 6 H, NCH_3) 7.3–7.8, 8.6–8.9 (m, C_6H_5, NH), 7.90 (s, H, CH).
(61) Petering, H. G.; Buskirk, H. H.; Underwood, G. E. *Cancer Res.* **1964**, *24*, 367–372.
(62) Bates, R. G.; Vega, C. A.; White, D. R. *Anal. Chem.* **1978**, *50*, 1295–1300.
(63) Green, M. A.; John, E. *J. Labeled Comp. Radiopharm.* **1989**, *26*, 351–353.
(64) Petering, D. H. *Bioinorg. Chem.* **1972**, *1*, 273–288.
(65) Petering, D. H. *Bioinorg. Chem.* **1972**, *1*, 255–271.
(66) Winkelmann, D. A.; Bermke, Y.; Petering, D. H. *Bioinorg. Chem.* **1974**, *3*, 261–277.
(67) Minkel, D. T.; Saryan, L. A.; Petering, D. H. *Cancer Res.* **1978**, *38*, 124–129.
(68) Minkel, D. T.; Petering, D. H. *Cancer Res.* **1978**, *38*, 117–123.
(69) (a) Robinson, G. D. *Prog. Nucl. Med.* **1978**, *4*, 80–92. (b) Robinson, G. D.; Zielinski, F. W.; Lee, A. W. *Int. J. Appl. Radiat. Isotopes* **1980**, *31*, 111–116.

Table II. Blood Levels of Tracer Copper Afforded by Copper Bis(thiosemicarbazone) Complexes in the Rat

	% injected dose in blood		
ligand	1 min	5 min	2 h
PTS	18. ± 4.	9.6 ± 0.9	7.9[a] ± 0.7
ETS	13.4 ± 2.9	10.0 ± 1.5	8.1 ± 0.7
KTS	15.8 ± 1.5	10.1 ± 0.7	7.0 ± 0.7
n-PrTS	15.2 ± 5.0	8.9 ± 1.1	8.5 ± 0.4
i-PrTS	10.7 ± 0.9	9.3 ± 0.8	6.7 ± 0.4
n-BuTS	8.4 ± 1.1	6.5 ± 0.3	6.3 ± 0.4
PhTS	13.4 ± 1.0	9.3 ± 0.7	7.1 ± 0.4
PTSM	9.3 ± 1.3	8.0 ± 1.7	7.5 ± 2.5
ETSM	7.3 ± 0.6	6.6 ± 0.5	6.5 ± 0.4
KTSM	7.5 ± 1.4	5.8 ± 0.1	6.2 ± 0.4
n-PrTSM	7.7 ± 0.5	6.4 ± 0.4	5.5 ± 0.3
i-PrTSM	7.1 ± 1.3	7.7 ± 1.3	8.3 ± 1.4
n-BuTSM	5.8 ± 0.2	5.8 ± 0.5	5.4 ± 0.2
PhTSM	12.8 ± 2.3	7.0 ± 0.3	6.6 ± 0.5
PTSE	8.5 ± 0.7	6.7 ± 0.1	5.2 ± 1.1
$PTSM_2$	5.9 ± 1.0	5.4 ± 0.5	5.2[b] ± 0.2
$ETSM_2$	6.3 ± 0.6	4.0 ± 0.3	7.3 ± 1.2
$KTSM_2$	5.1 ± 1.0	4.6 ± 1.6	6.6 ± 1.1

[a] 15 min. [b] 30 min.

Table III. Brain Levels of Tracer Copper Afforded by Copper Bis(thiosemicarbazone) Complexes in the Rat

	% injected dose in brain		
ligand	1 min	5 min	2 h
PTS	0.46 ± 0.15	0.29 ± 0.05	0.34[a] ± 0.09
ETS	0.71 ± 0.07	0.7 ± 0.2	0.86 ± 0.08
KTS	0.76 ± 0.10	0.75 ± 0.05	0.64 ± 0.15
n-PrTS	1.45 ± 0.33	1.27 ± 0.22	1.79 ± 0.22
i-PrTS	1.0 ± 0.1	1.1 ± 0.2	1.1 ± 0.1
n-BuTS	1.62 ± 0.46	1.37 ± 0.35	1.60 ± 0.24
PhTS	1.15 ± 0.03	1.29 ± 0.19	1.30 ± 0.19
PTSM	3.0 ± 0.7	3.0 ± 0.6	3.2 ± 0.4
ETSM	2.8 ± 0.4	2.7 ± 0.3	2.9 ± 0.3
KTSM	2.5 ± 0.5	2.5 ± 0.2	2.5 ± 0.3
n-PrTSM	3.1 ± 0.8	2.3 ± 0.1	2.2 ± 0.4
i-PrTSM	3.4 ± 0.5	2.9 ± 0.7	2.6 ± 0.7
n-BuTSM	2.4 ± 0.3	1.4 ± 0.2	1.7 ± 0.4
PhTSM	1.8 ± 0.5	1.3 ± 0.3	1.0 ± 0.1
PTSE	2.7 ± 0.6	1.8 ± 0.3	2.0 ± 0.3
$PTSM_2$	3.1 ± 0.4	2.2 ± 0.3	1.86[b] ± 0.06
$ETSM_2$	2.8 ± 0.3	1.6 ± 0.7	0.35 ± 0.07
$KTSM_2$	2.8 ± 0.4	2.1 ± 0.8	0.53 ± 0.10

[a] 15 min. [b] 30 min.

Table IV. Myocardial Levels of Tracer Copper Afforded by Copper Bis(thiosemicarbazone) Complexes in the Rat

	% injected dose in heart		
ligand	1 min	5 min	2 h
PTS	2.8 ± 0.4	2.3 ± 0.1	2.5[a] ± 0.4
ETS	3.2 ± 0.8	3.3 ± 0.9	3.0 ± 0.4
KTS	2.5 ± 0.5	2.7 ± 0.2	1.34 ± 0.15
n-PrTS	3.9 ± 1.6	3.0 ± 0.4	3.5 ± 0.6
i-PrTS	1.3 ± 0.1	1.2 ± 0.1	0.82 ± 0.05
n-BuTS	2.4 ± 0.3	2.3 ± 0.2	2.1 ± 0.3
PhTS	2.6 ± 0.2	2.7 ± 0.6	2.2 ± 0.3
PTSM	2.7 ± 0.3	3.4 ± 1.2	3.3 ± 0.9
ETSM	2.6 ± 0.4	2.7 ± 0.7	2.3 ± 0.3
KTSM	2.1 ± 0.4	1.7 ± 0.1	1.2 ± 0.2
n-PrTSM	2.4 ± 0.7	1.8 ± 0.5	1.4 ± 0.3
i-PrTSM	1.7 ± 0.8	1.5 ± 0.5	0.95 ± 0.26
n-BuTSM	1.7 ± 0.4	1.1 ± 0.2	1.4 ± 0.6
PhTSM	1.8 ± 0.6	0.87 ± 0.1	0.81 ± 0.2
PTSE	1.9 ± 0.2	1.7 ± 0.3	1.2 ± 0.2
$PTSM_2$	0.97 ± 0.15	0.43 ± 0.14	0.31[b] ± 0.02
$ETSM_2$	1.3 ± 0.2	0.35 ± 0.06	0.30 ± 0.07
$KTSM_2$	2.3 ± 0.2	0.57 ± 0.17	0.34 ± 0.04

[a] 15 min. [b] 30 min.

phase after the initial P measurement. While the second extraction occasionally gave a somewhat higher value for P, in all cases third extractions of the octanol phase gave a value of P identical with that measured in the second partitioning. The reported values of P (Table I) represent the values obtained in these second and third extractions and are the mean of six measurements. In examining the effects of functionalization on the lipophilicity of benzene derivatives, Hansch et al.[70] observed increases in log P by ca. 0.5–0.6 for each added $-CH_3$ or $-CH_2-$ fragment, a substituent effect comparable to what we observe for these copper chelate complexes. The lipophilicity of these copper compounds spans the $0.9 < \log P < 2.5$ range where Dischino et al.[31] observed complete cerebral extraction of ^{11}C-labeled alcohols and ethers. In addition, all of these copper bis(thiosemicarbazone) complexes fall below the molecular weight (M_r) of 400 where Levin observed increases in the brain capillary permeability coefficient (P_c) with increasing P for a relatively diverse collection of organic nonelectrolytes.[27]

The biodistribution of each copper-67 bis(thiosemicarbazone) complex was determined in rats following injection into the femoral vein. (Use of the exposed femoral vein for injection allows visual verification that the dose is quantitatively delivered intravenously.) The complexes all rapidly clear from the blood (Table II), but show large variations in cerebral and myocardial uptake and retention (Tables III and IV). In all cases the brain level of these tracers significantly exceeds that which could be attributed to blood-borne radioactivity (blood accounts for approximately 3% of rat brain mass[71]). The observed variations in ability to penetrate the blood–brain barrier, assessed by brain levels of tracer at 1 min postinjection,[72] correlate well with distinct structural features and physicochemical properties of the complexes. Alkylation of the terminal amino groups appears essential for good cerebral uptake of tracer. The N^4-alkylated complexes ($Cu[R_{(1)}TSM]$, $Cu[R_{(1)}TSE]$, and $Cu[R_{(1)}TSM_2]$) all efficiently cross the blood–brain barrier, with 2.5–3.0% of the injected dose found in the brain at 1 min postinjection (Table III). This compares favorably to the brain tracer levels observed shortly after intravenous administration of ^{11}C-labeled 1-butanol.[73] In contrast to the N^4-alkylated derivatives, the parent bis(thiosemicarbazone) complexes, $Cu[R_{(1)}TS]$, penetrate the blood–brain barrier rather poorly, although their brain uptake does increase with increasing lipophilicity over the $0.75 < \log P < 2.4$ range. The reason for the relatively low brain uptake of the $Cu[R_{(1)}TS]$ complexes is not readily apparent. We hypothesize that it may be related to the increased ability of the $Cu[R_{(1)}TS]$ complexes to act as hydrogen-bond donors, producing weak interactions with blood, water, and plasma proteins that reduce the diffusibility of the copper tracers. (None of these uncharged copper chelate complexes are expected to be protonated at blood or brain pH values, on the basis of reported acid dissociation constants.[65] In addition, we have previously reported electrophoresis studies of ^{67}Cu-labeled Cu[PTS], Cu[PTSM], and $Cu[PTSM_2]$ that also

(70) Fujita, T.; Iwasa, J.; Hansch, C. *J. Am. Chem. Soc.* **1964**, *86*, 5175–5180.

(71) Preston, E.; Allen, M.; Haas, N. *J. Neurosci. Meth.* **1983**, *9*, 45–55.

(72) A reviewer has correctly pointed out that this statement assumes the brain levels of tracer at 1 min following iv injection to reflect predominantly the unidirectional extraction. We believe this to be a reasonable assumption, having previously observed an excellent correlation between the brain levels of Cu[PTS], Cu[PTSM], and $Cu[PTSM_2]$ at 1 min postinjection (iv) and their respective brain uptake index (BUI) values.[33]

(73) Green, M. A.; Welch, M. J.; Mathias, C. J.; Fox, K. A. A.; Knabb, R. M.; Huffman, J. C. *J. Nucl. Med.* **1985**, *26*, 170–180.

Table V. Properties of Copper(II) Bis(thiosemicarbazone) Complexes[a]

complex	$E_{1/2}$ (V)[b]	k/k_0[c] (cells)	k/k_0 (dithiothreitol)
Cu[PTS]	−0.188	396	250
Cu[PTSM]	−0.208	434	250
Cu[$PTSM_2$]	−0.278	1.0	1.0
Cu[KTS]	−0.178	833	67
Cu[KTSM]	−0.188	358	56
Cu[$KTSM_2$]	−0.283	3.0	0.50

[a] From ref 67; k = pseudo-first-order rate constant for reaction with the specified reagent. [b] pH = 9.1. [c] Relative rates of reaction with Ehrlich cell suspension.

indicate these tracers to be uncharged at physiological pH.[33])

Although Dischino et al.[31] observed a decrease in the cerebral extraction of ^{11}C-labeled alcohols and ethers above log P = 2.5 at a cerebral blood flow (CBF) of 1.0 mL min^{-1} g^{-1}, in our series of copper compounds it would appear that cerebral extraction of the N^4-alkylated complexes does not fall off even for the most lipophilic tracers studied, Cu[$ETSM_2$] and Cu[$KTSM_2$] (log P values >3.2). Unfortunately, the reason for this apparent discrepancy can not be resolved with only the animal data currently available for the copper tracers. Clearly some caution must be exercised in quantitatively extrapolating Dischino's results to another animal model; the results presented here could indicate an inherent limitation in the generality of Dischino's structure–activity relationship when applied to structurally diverse molecules, or they might indicate that our animal model is not a sufficiently critical test of the diffusibility of these copper tracers between blood and brain. While determinations of compound biodistribution by the techniques described in this work provide a convenient and efficient means to screen potential new radiopharmaceuticals, this method (involving intravenous tracer injection) cannot realistically be expected to afford a great deal of sensitivity for making fine distinctions between the ability of various compounds to penetrate the BBB.

Discrete and consistent structural effects are also apparent in the rates of tracer clearance from the brain, a factor that seems to be largely independent of the initial brain uptake. The bis(thiosemicarbazone) ($R_{(1)}$TS) and bis(N^4-monoalkylthiosemicarbazone) ($R_{(1)}$TSM and $R_{(1)}$TSE) complexes always afford prolonged "microsphere-like" retention of tissue radiocopper, while the bis(N^4,N^4-dimethylthiosemicarbazone) ($R_{(1)}TSM_2$) complexes are always substantially cleared from the brain following their initial high uptake. The retention of cerebral activity afforded by the Cu[$R_{(1)}$TS] and Cu[$R_{(1)}$TSM] complexes is consistent with their known susceptibility to reductive decomposition by intracellular sulfhydryl groups,[64-68,74] a process that liberates ionic copper to be bound by intracellular macromolecules. The contrasting clearance of the Cu[$R_{(1)}TSM_2$] complexes is consistent with the known resistance of the copper(II) bis(N^4,N^4-dimethylthiosemicarbazones) to this redox process.[64-68]

Reduction potentials, relative rates of reaction with a tumor cell suspension, and relative rates of reaction with a model thiol (dithiothreitol) for six of these copper complexes are available from Petering's work to establish the mechanism for the antineoplastic activity of Cu[KTS].[64-68] The literature data in Table V shows the reduction potential of these molecules to be relatively insensitive to changes in the $R_{(1)}$ alkyl substituent, consistent with the expectation that the $-CH_3$ and $-CH(OEt)CH_3$ groups should be similar in electron-donating ability. As would

(74) Kraker, A.; Krezoski, S.; Schneider, J.; et al. *J. Biol. Chem.* **1985**, *260*, 13710–13718.

Table VI. Kidney Levels of Tracer Copper Afforded by Copper Bis(thiosemicarbazone) Complexes in the Rat

ligand	% injected dose in kidney (one) 1 min	5 min	2 h
PTS	3.7 ± 1.6	4.2 ± 1.7	5.0[a] ± 1.1
ETS	3.1 ± 0.4	2.6 ± 0.5	3.0 ± 0.5
KTS	2.7 ± 0.7	2.0 ± 0.4	2.8 ± 0.5
n-PrTS	2.8 ± 0.5	2.8 ± 0.8	3.6 ± 0.4
i-PrTS	2.5 ± 0.3	2.4 ± 0.15	3.0 ± 0.4
n-BuTS	2.8 ± 0.3	2.3 ± 0.4	2.6 ± 0.4
PhTS	2.9 ± 0.5	2.5 ± 0.6	2.9 ± 0.4
PTSM	3.7 ± 0.7	3.1 ± 0.1	4.3 ± 0.4
ETSM	2.3 ± 0.6	2.2 ± 0.6	2.2 ± 0.2
KTSM	2.6 ± 0.9	2.1 ± 0.5	2.7 ± 0.7
n-PrTSM	2.4 ± 0.7	2.0 ± 0.3	2.6 ± 0.5
i-PrTSM	2.5 ± 0.9	2.4 ± 0.4	3.1 ± 0.7
n-BuTSM	2.0 ± 0.7	1.6 ± 0.2	2.6 ± 0.3
PhTSM	2.7 ± 0.7	1.6 ± 0.2	2.5 ± 0.3
PTSE	3.0 ± 0.3	2.2 ± 0.2	4.6 ± 1.4
$PTSM_2$	1.8 ± 0.4	1.2 ± 0.2	2.3[b] ± 0.3
$ETSM_2$	1.7 ± 0.1	0.67 ± 0.09	2.2 ± 0.6
$KTSM_2$	2.6 ± 0.28	0.92 ± 0.29	2.0 ± 0.1

[a] 15 min. [b] 30 min.

Table VII. Liver Levels of Tracer Copper Afforded by Copper Bis(thiosemicarbazone) Complexes in the Rat

ligand	% injected dose in liver 1 min	5 min	2 h
PTS	7.8 ± 2.4	11.3 ± 2.2	13.1[a] ± 0.7
ETS	11.7 ± 1.3	14.0 ± 2.1	20.0 ± 3.1
KTS	9.7 ± 2.6	12.1 ± 2.0	14.7 ± 1.2
n-PrTS	11.5 ± 2.7	13.7 ± 3.8	17.3 ± 0.4
i-PrTS	11.1 ± 0.6	15.2 ± 0.7	15.0 ± 0.4
n-BuTS	10.0 ± 1.6	11.9 ± 1.1	13.3 ± 0.6
PhTS	12.6 ± 0.8	13.3 ± 1.1	13.7 ± 0.3
PTSM	12.5 ± 2.2	14.4 ± 1.0	15.6 ± 1.2
ETSM	9.9 ± 2.8	12.7 ± 2.8	12.8 ± 1.1
KTSM	10.1 ± 1.3	14.8 ± 0.7	13.9 ± 0.1
n-PrTSM	10.0 ± 3.9	16.9 ± 3.4	14.5 ± 1.3
i-PrTSM	17.2 ± 7.9	25.9 ± 7.7	19.2 ± 3.0
n-BuTSM	13.3 ± 7.1	19.3 ± 2.8	16.2 ± 2.0
PhTSM	24.6 ± 7.1	23.5 ± 5.8	16.6 ± 1.4
PTSE	14.5 ± 1.7	18.9 ± 1.5	19.1 ± 4.0
$PTSM_2$	11.2 ± 2.8	23.1 ± 3.6	21.5[b] ± 0.9
$ETSM_2$	18.2 ± 5.6	23.2 ± 3.2	18.7 ± 3.8
$KTSM_2$	25.2 ± 3.1	35.2 ± 6.6	21.9 ± 4.2

[a] 15 min. [b] 30 min.

Table VIII. Pulmonary Levels of Tracer Copper Afforded by Copper Bis(thiosemicarbazone) Complexes in the Rat

ligand	% injected dose in lungs 1 min	5 min	2 h
PTS	15. ± 4.	9.1 ± 1.8	7.4[a] ± 1.4
ETS	12.8 ± 1.7	11.0 ± 2.8	4.6 ± 1.0
KTS	15.1 ± 3.4	8.3 ± 0.6	3.3 ± 0.4
n-PrTS	13.1 ± 2.8	9.6 ± 1.1	5.2 ± 1.4
i-PrTS	7.7 ± 1.1	5.8 ± 2.1	2.1 ± 0.12
n-BuTS	12.2 ± 1.8	9.3 ± 1.7	3.4 ± 0.9
PhTS	11.1 ± 1.8	10.9 ± 1.7	4.0 ± 1.3
PTSM	8.2 ± 1.6	6.1 ± 0.9	4.0 ± 1.7
ETSM	4.7 ± 1.2	6.8 ± 2.5	1.8 ± 0.2
KTSM	15.0 ± 5.4	9.4 ± 2.0	3.9 ± 0.6
n-PrTSM	7.1 ± 0.9	6.3 ± 2.5	2.3 ± 0.2
i-PrTSM	3.4 ± 1.0	3.8 ± 1.2	1.7 ± 0.4
n-BuTSM	2.4 ± 0.5	2.0 ± 0.5	1.2 ± 0.4
PhTSM	4.9 ± 0.9	2.5 ± 0.6	1.4 ± 0.4
PTSE	7.4 ± 3.7	4.2 ± 1.5	1.7 ± 0.2
$PTSM_2$	4.8 ± 1.4	1.6 ± 0.5	1.3[b] ± 0.2
$ETSM_2$	2.6 ± 1.5	0.83 ± 0.08	0.69 ± 0.2
$KTSM_2$	1.46 ± 0.14	0.86 ± 0.27	0.75 ± 0.02

[a] 15 min. [b] 30 min.

be predicted, the complexes become more difficult to reduce ($E_{1/2}$ becomes more negative) with increasing substitution of electron-releasing alkyl groups onto the π-conjugated ligand backbone. Addition of the first pair of N^4-methyl substituents to the Cu[$R_{(1)}$TS] complexes decreases the reduction potential by 10–20 mV, while the second pair of N^4-methyl groups produces a dramatic decrease of 70–95 mV in the reduction potential. The relative rates at which these compounds react with cell suspensions or dithiothreitol are relatively constant, with the exception of the two bis(N^4,N^4-dimethylthiosemicarbazone) complexes, Cu[$PTSM_2$] and Cu[$KTSM_2$], which are comparatively inert. In this regard, it is of interest to note that the most abundant source of -SH in the cell, glutathione, has a reduction potential of -0.23 V (pH 7),[75] intermediate between those of the bis(N^4,N^4-dimethylthiosemicarbazone) complexes and their less highly alkylated derivatives. The reactivity of this series of six complexes towards cells (i.e. their tendency to deposit ionic copper inside cells) is thus reasonably correlated with their ability to be reduced by intracellular glutathione (assuming the copper complex redox potentials are relatively insensitive to pH). Since each structural modification in these six ligands produces a distinct and consistent effect on both the redox potential of the Cu^{II} complex and its reactivity towards thiols, we can be reasonably confident in the extrapolation of these trends to the other copper bis(thiosemicarbazone) complexes we have studied for which no electrochemical or kinetic data are now available. The copper(II) bis(thiosemicarbazone) complexes that are expected to be kinetically reactive do appear to be reductively decomposed to afford tracer trapping in brain tissue, while the kinetically inert complexes are instead cleared from the brain. The addition of bulky groups to the bis(N^4-monoalkylthiosemicarbazone) complexes does tend to reduce their cerebral retention (note Cu[*i*-PrTSM], Cu[*n*-PrTSM], Cu[*n*-BuTSM], and Cu[PTSE]), possibly because steric hindrance about the metal center impairs the approach of the sulfhydryl reductant.[66]

Myocardial levels of tracer copper are presented in Table IV for the series of copper bis(thiosemicarbazone) complexes studied. As in the brain, the Cu[$R_{(1)}$TS] and Cu[$R_{(1)}$TSM] complexes yield microsphere-like retention of myocardial radiocopper, while the Cu[$R_{(1)}TSM_2$] complexes are substantially cleared. It is of interest to note that the myocardial levels of tracer afforded by the Cu[$R_{(1)}$TS] complexes are comparable to those of the Cu[$R_{(1)}$TSM] derivatives. Thus, the low brain uptake of the Cu[$R_{(1)}$TS] complexes relative to their N^4-methyl derivatives does not appear to result from differences in binding to blood components, which we would expect to reduce both cerebral and myocardial extraction, but must instead reflect intrinsic differences in their ability to penetrate the blood–brain barrier. Unlike in the brain, there is a significant difference between the myocardial levels of radiocopper that result shortly after injection of the bis(N^4-monomethyl) and bis(N^4,N^4-dimethyl) derivatives of either pyruvaldehyde or ethylglyoxal. In both cases the bis(N^4,N^4-dimethyl) complexes show substantially lower myocardial uptake at 1 min postinjection than the bis(N^4-monomethyl) complexes. The reasons for this are unclear, but it does not appear to simply result from the greater lipophilicity of the bis(N^4,N^4-dimethyl) complexes, since Cu[$KTSM_2$] does provide relatively high myocardial levels of tracer at 1 min postinjection. Simply on the basis of the relative levels of myocardial tracer uptake, none of the compounds studied would appear to be more promising than Cu[PTSM] for myocardial imaging.

Biodistribution data is presented in Tables VI–VIII for the kidney, liver, and lungs. As should be expected, tissue trapping of those tracers susceptible to intracelluar redox processes is not limited to the brain and heart. In this regard, glutathione is quite attractive as a reagent for inducing the tissue trapping of tracer copper since it is both ubiquitous and abundant in mammalian cells, occurring in millimolar concentrations in cells yet only in micromolar concentrations in plasma.[76,77] The observed clearance of >90% of even the reactive copper(II) bis(thiosemicarbazones) from blood must be attributed, at least in part, to the relatively low concentrations of glutathione in plasma relative to other tissues. (If ionic copper-67 was being rapidly released in plasma, the distribution of tracer would be dramatically different from that actually observed.[32]) The lungs are the only organ to exhibit significant clearance of the C[$R_{(1)}$TS] and Cu[$R_{(1)}$TSM] complexes beyond 1 min postinjection. We attribute tracer clearance from the lungs, at least in part, to the very high rates of pulmonary blood flow relative to other organs.[78] The data obtained for Cu[KTS] agrees reasonably well with that reported by other workers in mouse and tumor rat models[79,80] and suggests that for many organs the tissue distribution of therapeutic levels of this antineoplastic agent will be perfusion rate limited.

Conclusions

The studies reported here support the hypothesis that the microsphere-like tissue retention of tracer copper afforded by Cu[PTSM] can be attributed to reductive decomposition of the copper chelate by intracellular sulfhydryl groups. For nuclear medicine imaging applications that frequently require tissue trapping of tracer we appear fortunate in that the kinetics of this redox process are sufficiently slow to allow radiopharmaceutical delivery to organs of interest, while still being sufficiently rapid that excessive clearance of extracted tracer does not occur prior to its reductive decomposition to liberate ionic copper. Studies are continuing to better define both the potential clinical application of these copper tracers as diagnostic imaging agents and the chemical fate of the copper radiolabel.

Acknowledgment. This work was supported by grants from the National Heart, Lung, and Blood Institute (Grant No. K04-HL01801), the National Cancer Institute (Grant No. RO1-CA46909), and the NIH Biomedical Research Support Grant Program (Grant No. S07-RR05586). The authors thank Ingrid D. Baerga for technical assistance in some of the rat biodistribution studies.

Supplementary Material Available: Tables IX–XXVI presenting rat biodistribution data calculated as percent injected dose/gram organ wet weight for each of the compounds and time points studied (9 pages). Ordering information is given on any current masthead page.

(75) Mahler, H.; Cordes, E. H. *Biological Chemistry*; Harper and Row: New York, 1971; pp 30.

(76) (a) Meister, A.; Anderson, M. E. *Annu. Rev. Biochem.* **1983**, *52*, 711–760. (b) Anderson, M. E.; Meister, A. *J. Biol. Chem.* **1980**, *255*, 9530–9533.

(77) Long, C., Ed.; *Biochemist's Handbook*, D. Van Nostrand: Princeton, N.J., 1961; pp 793–795.

(78) Welling, P. G. *Pharmacokinetics*; American Chemical Society: Washington, D.C., 1986; pp 80–82.

(79) Pastakia, B.; Zieberman, L. M.; Gatley, S. J.; Young, D.; Petering, D. H.; Minkel, D. *J. Nucl. Med.* **1980**, *21*, 67–70.

(80) (a) Hosotani, T.; Yokoyama, A.; Arano, Y.; Horiuchi, K.; Wasaki, H.; Saji, H.; Torizuka, K. *Int. J. Nucl. Med. Biol.* **1986**, *12*, 431–437. (b) Yokoyama, A.; Hosotani, T.; Arano, Y.; Horiuchi, K. *Radioisotopes (Japan)* **1986**, *35*, 249–255.